Available online at www.sciencedirect.com
ScienceDirect
Journal of Catalysis 253 (2008) 11–21
JOURNAL OF CATALYSIS
www.elsevier.com/locate/jcat

Zn-promoted hydrogen exchange for methane and ethane on Zn/H-BEA zeolite: In situ ^{1}H MAS NMR kinetic study

Alexander G. Stepanov [a,*], Sergei S. Arzumanov [a], Anton A. Gabrienko [b], Alexander V. Toktarev [a], Valentin N. Parmon [a], Dieter Freude [c,*]

[a] *Boreskov Institute of Catalysis, Siberian Branch of the Russian Academy of Sciences, Prospekt Akademika Lavrentieva 5, Novosibirsk 630090, Russia*
[b] *Department of Natural Sciences, Novosibirsk State University, Pirogova Street 2, Novosibirsk 630090, Russia*
[c] *Universität Leipzig, Abteilung Grenzflächenphysik, Linnéstraße 5, 04103 Leipzig, Germany*

Received 18 July 2007; revised 19 October 2007; accepted 3 November 2007

Abstract

Hydrogen (H/D) exchange between Brønsted acid sites of both the acidic form of zeolite beta (H-BEA) and Zn-loaded zeolite beta (Zn/H-BEA) and small alkanes (methane and ethane) has been studied by monitoring the kinetics of the exchange in situ with ^{1}H MAS NMR spectroscopy within the temperature range of 433–563 K. On Zn/H-BEA, the exchange has been found to be more than two orders of magnitude faster compared to that on H-BEA. The decrease of reaction temperature and activation energy of the exchange on Zn/H-BEA (86–88 kJ mol^{-1}) compared to the acidic form of zeolite H-BEA (138 kJ mol^{-1}) has been rationalized by the promoting effect of zinc. We propose that the mechanism of the H/D exchange on Zn/H-BEA involves Zn-alkyl species as intermediates.

Keywords: Methane; Ethane; Zn/H-BEA zeolite; H/D exchange; Kinetics; Promoting effect; ^{1}H MAS NMR spectroscopy

1. Introduction

Zn-modified zeolites are effective catalysts for light alkanes aromatization [1–4]. The enhanced selectivity of alkane conversion (ethane [5–7] and propane [8,9]) towards aromatics is attributed to dehydrogenation ability of the loaded zinc species. It has been claimed [2,3] that strong Lewis sites, which are generated by zinc, change the mechanism of alkane activation and transformation from the beta scission to a dehydrogenation step. The alkenes formed under dehydrogenation then undergo a dehydrocyclooligomerization. Both Brønsted acid sites and Zn sites are involved in dehydrocyclooligomerization and produce finally the aromatic compounds [3,8,10,11].

Kazansky et al. [12–14] demonstrated the formation of strong adsorption complexes between small alkanes and Zn^{2+} cations by IR spectroscopy. They claimed that the activation of the alkane molecules in zeolite occurred on Zn^{2+} cations. But a combined IR and NMR study by Ivanova et al. [15] indicated that the activation could alternatively occur on small ZnO clusters, which were located in the pores of the zeolite. Formation of Zn-alkyl species during alkane activation has been reported in both cases [12–15].

The role of possibly formed Zn-alkyl species, as well as the Brønsted acid sites, in small alkane activation requires further clarification. A reaction of hydrogen H/D exchange between acid sites of the zeolite and alkane molecule could help to establish the mechanism of alkane activation on Zn-loaded zeolites. Indeed, a hydrogen exchange between the acid sites of solid catalysts and alkane molecules, which precedes usually the chemical transformation of alkane on acid catalysts [16], is often used to characterize the activation of alkanes and acidity of the catalysts [17–28]. A combination of experimental H/D exchange kinetics data with theoretical analysis of the possible intermediates of the exchange reaction provides valuable information on the mechanisms of the alkane molecule activation and the H/D exchange on solid acid catalysts [17–19]. In this

* Corresponding authors. Fax: +49 341 97 39349.
E-mail addresses: stepanov@catalysis.ru (A.G. Stepanov), freude@uni-leipzig.de (D. Freude).

0021-9517/$ – see front matter
doi:10.1016/j.jcat.2007.11.002

paper, we consider the hydrogen H/D exchange between small alkanes (methane and ethane) and Brønsted acid sites of both Zn-loaded zeolite beta (Zn/H-BEA) and its pure acidic form (H-BEA).

2. Experimental

2.1. Materials characterization and samples preparation

The acidic form of the zeolite beta (H-BEA) (Si/Al = 18, average crystal size 0.1–0.2 μm) was synthesized using tetraethyl-ammonium hydroxide as template with subsequent calcination at 823 K in an air flow for 6 h [29]. Chemical analysis yielded the chemical composition: $Na_{0.475}H_{2.845}Al_{3.32}Si_{60.68}O_{128}$.

Zinc-loaded zeolite beta (Zn/H-BEA) was prepared by impregnation of the zeolite H-BEA with a saturated solution of zinc formate, subsequent drying at 473 K for 14 h and further calcination at 673 K for 4 h in a flow of air. The Zn content in the obtained zeolite Zn/H-BEA was 7.2 wt%. Zeolites were characterized by XRD, SEM, TEM, UV–vis and IR diffuse reflectance spectroscopy, and ^{1}H, ^{27}Al, ^{29}Si MAS NMR spectroscopy. A silicon-to-aluminum ratio of 18 in the zeolite framework obtained by ^{29}Si MAS NMR analysis [30], was in agreement with chemical analysis. The ^{27}Al MAS NMR spectrum exhibited only a signal at 54 ppm due to tetra-coordinated framework aluminum atoms for both H-BEA and Zn/H-BEA samples. The residual quantity of the acidic SiOHAl groups in a final Zn/H-BEA was 320 μmol g^{-1}, whereas the quantity of these groups was 480 μmol g^{-1} in the parent zeolite H-BEA. Concentrations of the acidic groups were obtained by the analysis of the intensities of signals of SiOHAl groups in ^{1}H MAS NMR spectra of Zn/H-BEA or H-BEA by comparing their intensities with that of methane as internal standard.

XRD analysis has demonstrated the presence of bulk ZnO phase in Zn/H-BEA. UV–vis diffuse reflectance spectrum of Zn/H-BEA exhibits the bands at 265 and 370 nm due to subnanometric ZnO clusters inside zeolite pores and due to macrocrystalline particles of ZnO on the external surface of the zeolite, respectively [31].

Methane-d_4 (99% D) and ethane-d_6 (99% D) purchased from Aldrich Chemical Company Inc. were used without further purification. The samples for NMR measurements were prepared by heating 80 mg of the zeolite sample in the glass tubes of 5.5 mm outer diameter. The samples were activated by an increase of the temperature from 300 to 673 K at the rate of 10 K h^{-1} under vacuum. Further, the samples were maintained at 673 K for 24 h under vacuum (less than 10^{-2} Pa). The loading was performed at room temperature with 1.15 molecules (ca. 300 μmol g^{-1}) of alkane per unit cell and each sample was then sealed off (length of the glass tube = 10 mm). This glass tube could be tightly inserted in 7 mm zirconia rotors. Before acquisition of the signal, the NMR probe with the sample was preheated for 20 min at the temperature at which the H/D exchange did not yet occur at notable rate. This temperature was 400 K for Zn/H-BEA and 473 K for H-BEA zeolite samples, respectively. Then the temperature was rapidly increased within 3–10 min by 40–100 K to the reaction temperature, equilibrated for 1–2 min, and then the acquisition of NMR signal started. It should be noted here that any noticeable chemical conversion of methane or ethane did not occur under conditions of our experiment, so the H/D exchange was the main transformation of the alkanes.

2.2. NMR measurements

NMR spectra were recorded at 9.4 T on a Bruker Avance-400 spectrometer equipped with high temperature broad-band double-resonance MAS probe. Zirconia rotors (7 mm outer diameter) with the inserted sealed glass tube were spun at 3–5 kHz by dried compressed air at 300–568 K. ^{1}H MAS spectra were recorded by the Hahn-echo pulse sequence ($\pi/2$–τ–π–τ–acquire), where τ equals to one rotor period (200–333 μs). The excitation pulse length was 4.5 μs ($\pi/2$), and typically 6–24 scans were accumulated with a 6–26 s delay. In double-resonance ^{1}H{^{27}Al} TRAPDOR experiments [32,33] a Hahn-echo sequence was applied to the ^{1}H channel with irradiation of aluminum during the both τ periods. The ^{27}Al nutation frequency of the irradiation field was about 70 kHz. ^{27}Al MAS spectra were acquired with a short $\pi/12$ radio-frequency pulse (0.6 μs), and about 1000 scans were accumulated with a 0.5 s recycle delay. ^{29}Si MAS spectra were recorded with $\pi/2$ excitation pulse of 5.0 μs duration, and 10–15 s repetition time, and 1000 scans for signal accumulation. Both ^{27}Al and ^{29}Si NMR spectra were recorded using 4 mm rotors and a spinning rate of 10 kHz. The chemical shifts were referenced to TMS for ^{1}H and ^{29}Si NMR and to 0.1 M $Al(NO_3)_3$ solution for ^{27}Al NMR. The sample temperature was controlled by the Bruker BVT-2000 variable-temperature unit. The calibration of the temperature inside the rotor was performed with an accuracy of ±2 K by using lead nitrate, located inside the rotor, as a ^{207}Pb MAS NMR chemical shift thermometer [34].

2.3. IR measurements

IR spectra were recorded on a Bruker Vector 22 FTIR spectrometer with a DTGS detector and 2 cm^{-1} resolution and 50 scans for signal accumulation. Zeolite samples were pressed in self-supporting discs (diameter: 1.5 cm, 10–20 mg cm^{-2}) and activated in the IR cell, attached to a vacuum line, at 723 K for 2 h at 10^{-2}–10^{-3} Pa. The adsorption of CO for testing the Lewis acidity was performed at 77 K at 13–1333 Pa CO pressure. Assessment of Lewis acidity was performed on the base of the absorbance bands at 2170–2230 cm^{-1} belonging to CO coordinated to Lewis site [35]. Among the bands observed for Zn/H-BEA at 2170–2230 cm^{-1}, the band at 2212 cm^{-1} was attributed to CO coordinated to isolated Zn^{2+} cations, the band at 2190 cm^{-1} to CO coordinated to small ZnO clusters and the band at 2170 cm^{-1} to CO on bulk ZnO phase. Quantitative estimations of Lewis sites in accordance to procedure described in Ref. [35] have shown that concentration of Lewis acid sites was ca. 30 μmol g^{-1} for H-BEA and ca. 110 μmol g^{-1} for Zn/H-BEA.

3. Results

3.1. Characteristics of hydroxyl groups of the H-BEA and Zn/H-BEA with IR and NMR

The IR spectrum of OH groups of H-BEA zeolite exhibits well-known [36–46] five signals, see Fig. 1. The signal at 3745 cm^{-1} belongs to the terminal and internal at framework defects SiOH groups. The signal at 3610 cm^{-1} is due to strongly acidic bridging hydroxyl groups. The broad band at 3600–3300 cm^{-1} is assigned to bridged hydroxyls which are perturbed by H-bond interactions with the zeolitic framework [43,45]. The signal at 3660–3680 cm^{-1} belongs to the acid OH groups connected to Al partially attached to the framework and located on external surfaces [37,38]. The band at 3790 cm^{-1} is attributed to low-acidity OH groups bonded to extra-lattice aluminum [37,39]. Similar bands are observed for Zn/H-BEA.

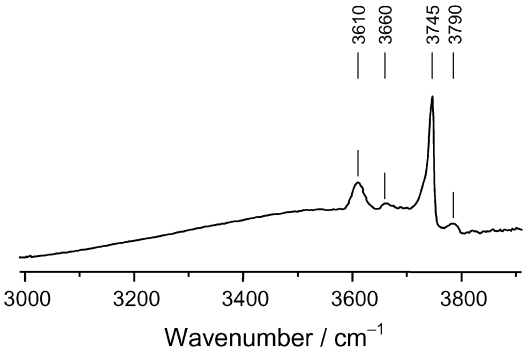

Fig. 1. IR spectrum of zeolite H-BEA.

^{1}H MAS NMR spectra of both H-BEA and Zn/H-BEA show three main signals, see Fig. 2. The signals at 4.0 and 5.1 ppm are due to the free bridged and hydrogen-bonded bridged hydroxyls (SiOHAl), respectively, and the most intense signal at 1.7 ppm arises from SiOH groups at framework defects and external SiOH groups [40,41,44,45]. The intense signal of SiOH groups is a result of the faulted structure of the zeolite beta (BEA) [47,48]. ^{1}H{^{27}Al} spin-echo double resonance (TRAPDOR [32,33]) experiments show the suppression of signals of protons that are not far from the next aluminum atom like SiOHAl or AlOH groups, while signals of protons far to the next aluminum atom are unaffected. On-resonance ^{27}Al irradiation for one rotor period (200–333 μs) results in a loss of intensity of three resonances in the ^{1}H{^{27}Al} MAS NMR spectrum of the zeolite H-BEA (Fig. 2b). The difference spectrum (Fig. 2c) shows four clearly distinguishable resonances at 5.1, 4.0, 2.6 and 1.0 ppm for H-BEA and a similar spectrum for Zn/H-BEA. The TRAPDOR difference spectrum strongly supports the IR data on the presence of two types of the OH groups associated with non-framework aluminum species. The signal at 2.6 ppm corresponds to the band at 3660–3680 cm^{-1}, and the signal at 1.0 ppm to the band at 3790 cm^{-1}.

The ^{27}Al MAS NMR spectrum of as-synthesized H-BEA exhibited only the signal of the framework aluminum atoms at 54 ppm. But the formation of a small quantity of extra-framework aluminum can occur during the sample activation under vacuum. Samples of H-BEA and Zn/H-BEA, which were first activated at 670 K and then rehydrated, contained a small amount of extra-framework aluminum species, which gave rise to a weak signal (a few percent with regards to the signal intensity at 54 ppm) at 5 ppm. Extra-framework aluminum species in the activated but not rehydrated sample can build AlOH groups,

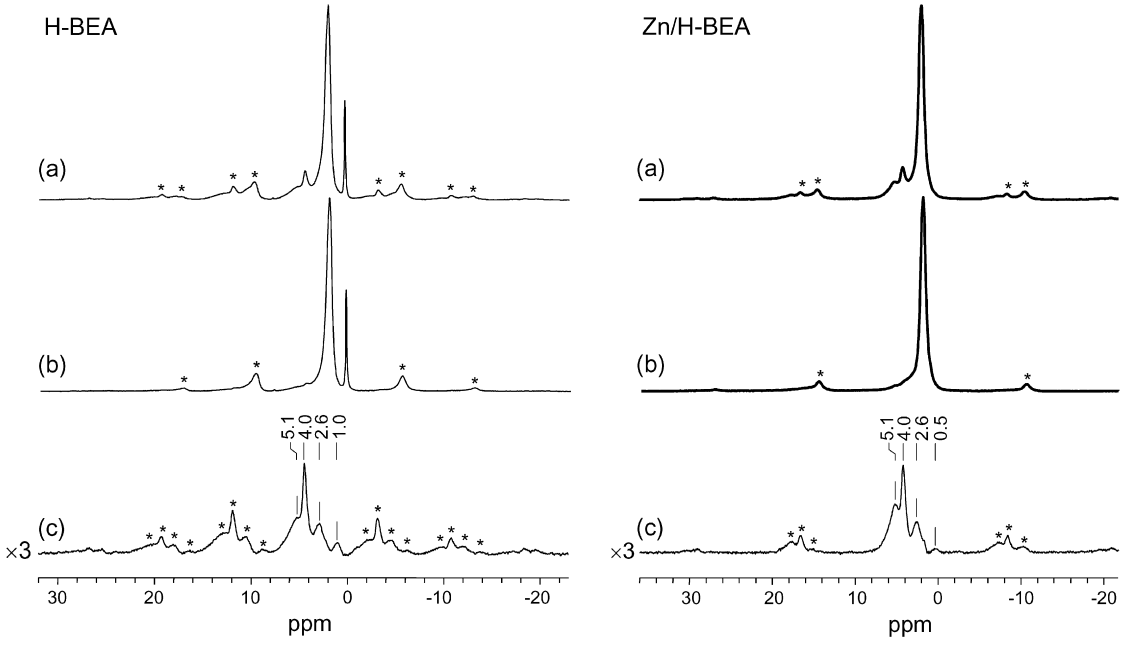

Fig. 2. ^{1}H MAS NMR room temperature Hahn-echo spectra of zeolites H-BEA and Zn/H-BEA activated under vacuum at 670 K: (a) without ^{27}Al irradiation, (b) with ^{27}Al irradiation (on resonance). The difference spectrum of (a) and (b) is shown in (c). The spinning speed was set to 3 kHz for H-BEA and 5 kHz for Zn/H-BEA, and τ was equal to one rotor period. Zeolite H-BEA was loaded with CD_4, which exhibited a residual protium signal at 0.0 ppm. Asterisks (*) belong to the spinning sidebands.

which give a signal at 1.0 ppm in the ^{1}H MAS NMR spectrum of dehydrated sample (Fig. 2). This means that a small quantity of extra-framework aluminum is created during the sample activation under vacuum.

3.2. Which OH groups of the zeolites are involved in the exchange?

During the H/D exchange between zeolitic OH groups and fully deuterated alkane molecules, the intensities of OH groups involved in the reaction should decrease, while the intensity of the alkane molecule signals increases in the ^{1}H MAS NMR spectrum. Fig. 3 shows the ^{1}H MAS NMR spectra of H-BEA with adsorbed CD_4 recorded before and after H/D exchange. The negative peaks in the difference spectrum (Fig. 3c) belong to the OH groups of the zeolite which are involved in the exchange. It is evident that both the acidic SiOHAl groups with chemical shift of 4.0–5.1 ppm and non-acidic SiOH groups with the chemical shift of 1.7 ppm are involved in the H/D exchange. For Zn/H-BEA both SiOHAl and SiOH groups are involved in the exchange as well. The experiments by Kramer et al. [17] on the pure-silica form of MFI, which contains no bridging OH groups, have shown that silanol groups are not active in the H/D exchange process. The simultaneous replacement of silanol and acidic hydroxyl groups by deuterium in acidic zeolite was attributed to an intra-zeolite exchange of hydrogen, possibly assisted by trace amounts of water [49,50]. In the present study, the observed involvement of SiOH of the zeolites H-BEA and Zn/H-BEA in the exchange (Fig. 3) should be attributed to more rapid exchange between zeolite SiOH and SiOHAl groups, compared to the H/D exchange between hydrogens of SiOHAl groups and the alkane molecules.

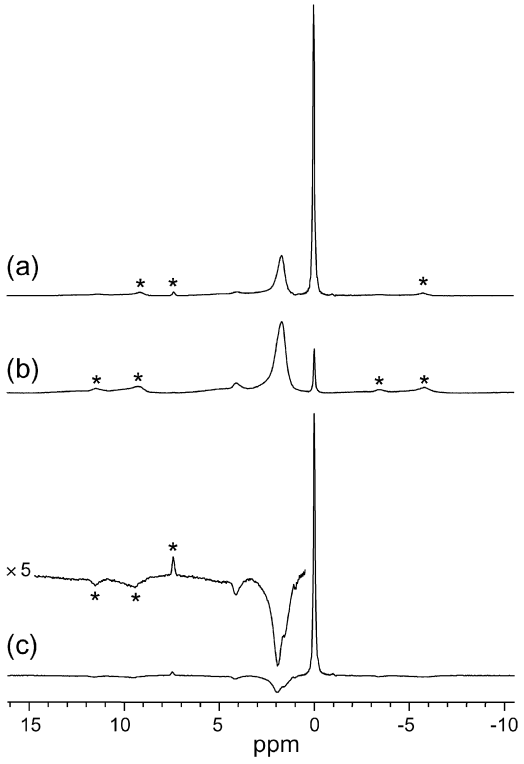

Fig. 3. ^{1}H MAS NMR room temperature Hahn-echo spectra of zeolite H-BEA with adsorbed methane-d_4 before (b) and after (a) reaction of H/D exchange at 563 K, (c) is the difference spectrum (a–b). The signal at 0.0 ppm in (b) corresponds to the residual protium in 99% deuterium enriched methane-d_4. Asterisks (*) denote the spinning sidebands.

3.3. Kinetics model

The kinetics of the exchange was analyzed assuming a parallel scheme of H/D exchange. In this scheme, all deuterium atoms in alkane exchange consecutively by the protium of the SiOHAl groups. In parallel, there is also a hydrogen exchange between SiOHAl and SiOH groups. Reactions (R1)–(R5) in Table 1 were used for modeling the H/D exchange of methane-d_4. Reactions (R1)–(R4) describe a consecutive exchange with SiOHAl groups. Reaction (R5) takes into account a transfer of hydrogen atoms between SiOHAl and SiOH groups. In a similar manner, the Reactions (R6)–(R12) describe the exchange of SiOHAl groups with both ethane-d_6 and SiOH groups. For each of the alkanes under study, the reaction rate constants were assumed to be equal for all consecutive stages of the exchange of the SiOHAl groups with alkane, i.e., the rate constants k_{SiOHAl} were similar for the Reactions (R1)–(R4) or the Reactions (R6)–(R11).

The reaction of isotopic substitution in a general form is

$$\mathrm{CD}_k\mathrm{H}_{a-k} + \mathrm{SiOHAl} \leftrightarrows \mathrm{CD}_{k1}\mathrm{H}_{a-k1} + \mathrm{SiODAl}, \tag{1}$$

where C designates carbon atoms in alkane molecule, a is the total contents of hydrogen isotopes in alkane molecule and k and $k1$ are the contents of deuterium in alkane. For a binomial distribution of isotopes under the exchange [26,51], the equilibrium constants K_{eq} (Table 1) are

$$K_{\mathrm{eq}} = \frac{\binom{a}{k1}}{\binom{a}{k}} \quad \text{with } \binom{a}{k} = \frac{a!}{k!(a-k)!}. \tag{2}$$

The kinetic scheme does not take into account the formation of penta-coordinated carbon atom of the alkane or zinc-alkyl fragment, which will be further discussed as the intermediates of the exchange reaction. The formation and expenditure of penta-coordinated carbon atom of alkane or zinc alkyl species can be fast and their concentration is low, so the kinetic scheme for the exchange reactions (Table 1) reflects only a direct exchange of OH groups and the hydrogen atoms of the alkane molecules. For intra-zeolite exchange (Reactions (R5) and (R12) in Table 1) a possible assistance of exchange by water traces is not reflected in kinetic schemes as well.

For the simulation of the experimental kinetic data we used a static model [52]:

$$\frac{\mathrm{d}N_i}{\mathrm{d}t} = \sum_{j=1}^{l} \nu_{ji} R_j, \tag{3}$$

where index i denotes different participants in the exchange reaction, i.e., the SiOHAl and SiOH groups of the zeolite (OH and OD), isotopomeric forms of methane $\mathrm{CD}_m\mathrm{H}_{4-m}$ ($m = 0$–4), or ethane $\mathrm{C_2D}_n\mathrm{H}_{6-n}$ ($n = 0$–6). N_i is the concentration of the component i (μmol g^{-1}). The stoichiometric coefficient of the

Table 1
Exchange reactions used for modeling the kinetics of the H/D exchange for methane and ethane on H-BEA and Zn/H-BEA

Reaction number	Exchange reaction	Equilibrium constant K_{eq}[a]	Rate constant k
	Methane		
(R1)	$CD_4 + SiOHAl \leftrightarrows CD_3H + SiODAl$	4	k_{SiOHAl}
(R2)	$CD_3H + SiOHAl \leftrightarrows CD_2H_2 + SiODAl$	3/2	k_{SiOHAl}
(R3)	$CD_2H_2 + SiOHAl \leftrightarrows CDH_3 + SiODAl$	2/3	k_{SiOHAl}
(R4)	$CDH_3 + SiOHAl \leftrightarrows CH_4 + SiODAl$	1/4	k_{SiOHAl}
(R5)	$SiOH + SiODAl \leftrightarrows SiOD + SiOHAl$	1	k_{intra}
	Ethane		
(R6)	$C_2D_6 + SiOHAl \leftrightarrows C_2D_5H + SiODAl$	6	k_{SiOHAl}
(R7)	$C_2D_5H + SiOHAl \leftrightarrows C_2D_4H_2 + SiODAl$	5/2	k_{SiOHAl}
(R8)	$C_2D_4H_2 + SiOHAl \leftrightarrows C_2D_3H_3 + SiODAl$	4/3	k_{SiOHAl}
(R9)	$C_2D_3H_3 + SiOHAl \leftrightarrows C_2D_2H_4 + SiODAl$	3/4	k_{SiOHAl}
(R10)	$C_2D_2H_4 + SiOHAl \leftrightarrows C_2DH_5 + SiODAl$	2/5	k_{SiOHAl}
(R11)	$C_2DH_5 + SiOHAl \leftrightarrows C_2H_6 + SiODAl$	1/6	k_{SiOHAl}
(R12)	$SiOH + SiODAl \leftrightarrows SiOD + SiOHAl$	1	k_{intra}

[a] $K_{eq} = \frac{k_{SiOHAl}}{k_{r1}}$ or $\frac{k_{intra}}{k_{r2}}$, where k_{r1} and k_{r2} are the rate constants of the reverse reactions for Eqs. (R1)–(R12).

component i in the reaction j is denoted as ν_{ji}. For methane and ethane we have the values $l = 5$ and 7, respectively. R_j is the rate of the reaction j, which is determined as

$$R_j = k_j N_{i1} N_{i2} \left(1 - \frac{N_{k1} N_{k2}}{K_{eq} N_{i1} N_{i2}}\right), \tag{4}$$

where k_j is the rate constant, N_{i1}, N_{i2} are the concentrations of reagents, and N_{k1}, N_{k2} denote the concentrations of products in the reaction j.

In order to solve Eq. (3), the normalization conditions and the initial conditions should be used. The initial conditions are

$$N_i(t = 0) = N_i^0. \tag{5}$$

The normalization conditions (e.g., for methane) are

$$\begin{aligned}
&[SiOHAl] + [SiODAl] = N^0_{SiOHAl},\\
&[SiOH] + [SiOD] = N^0_{SiOH},\\
&\sum_{m=0}^{4} [CD_mH_{4-m}] = N^0_{CH_4}.
\end{aligned} \tag{6}$$

The semi-implicit Runge–Kutta method [53] for integration of sets of stiff equations with an integration step adaptation was used to solve the system of differential equations (3). Thus the concentrations of all components N_i in dependence on the reaction time could be determined. The concentrations of protium in the alkane molecules and OH groups (intensities of the correspondent signals in the ^{1}H NMR spectrum) were calculated by the equations

$$\begin{aligned}
&\sum_{m=0}^{3} (4-m)[CD_mH_{4-m}] = [H]_{CH_4} \propto I_{CH_4},\\
&\sum_{n=0}^{5} (6-n)[C_2D_nH_{6-n}] = [H]_{C_2H_6} \propto I_{C_2H_6},\\
&[SiOHAl] = [H]_{SiOHAl} \propto I_{SiOHAl},\\
&[SiOH] = [H]_{SiOH} \propto I_{SiOH}.
\end{aligned} \tag{7}$$

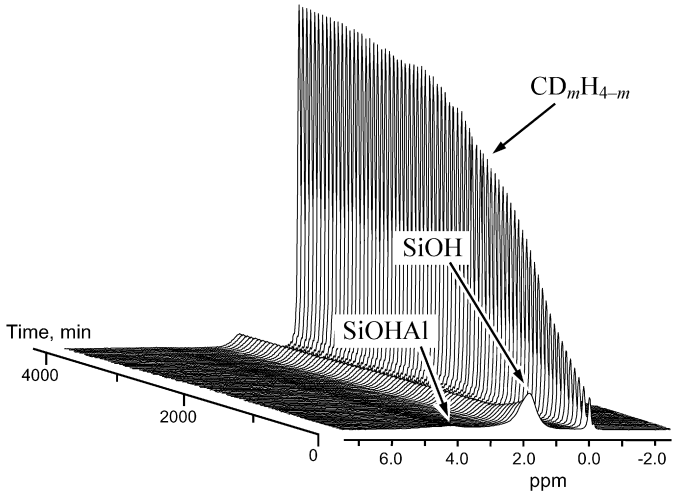

Fig. 4. Stack plot of the ^{1}H MAS NMR spectra at 558 K of methane-d_4 adsorbed on H-BEA. The first spectrum (bottom) was recorded 5 min after the temperature was raised and equilibrated at 558 K and the last spectrum (top) after 4110 min of the reaction duration. The time between subsequent spectra recording was 60 min.

The rate constants k_{SiOHAl} and k_{intra} were determined by fitting the experimentally obtained concentrations of protium in methane ($[H]_{CH_4}$) or ethane ($[H]_{C_2H_6}$), SiOHAl ($[H]_{SiOHAl}$) and SiOH ($[H]_{SiOH}$). Accuracies of the rate constants were in the range of 10–40% as determined from the spread of the experimental points on the kinetic curves.

3.4. H/D exchange of methane-d_4 on zeolite H-BEA

Fig. 4 shows the ^{1}H MAS NMR spectra of methane-d_4 adsorbed on zeolite H-BEA in dependence on reaction time. An increasing signal at 0.0 ppm belongs to methane CD_mH_{4-m} ($m = 0$–3). Two decreasing signals at 4.0 and ca. 5.1 ppm arise from SiOHAl groups. The signal at 1.7 ppm has mainly a contribution from terminal SiOH groups and decreases also with the reaction time. The growth of the signal at 0.0 ppm and simultaneous decrease of the signals at 4.0, 5.1 and 1.7 ppm is

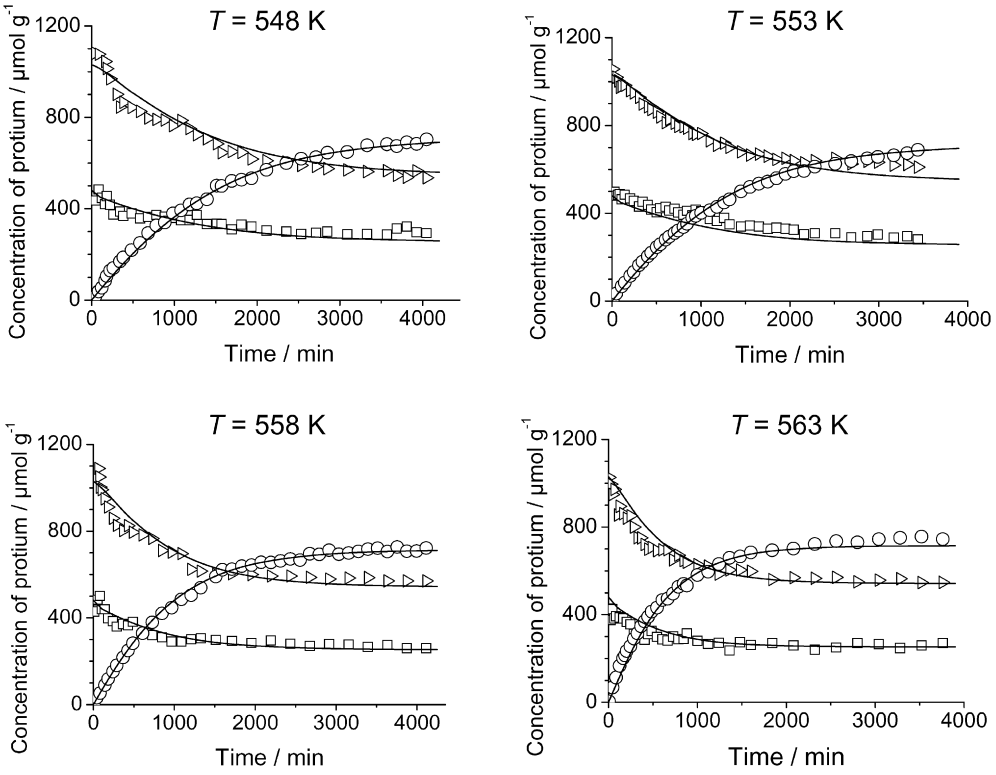

Fig. 5. Experimental and simulated (solid curves) kinetics of the H/D exchange for methane-d_4 on H-BEA. Simulation was performed in accordance to parallel kinetic scheme of the H/D exchange between SiOHAl and methane and between SiOHAl and SiOH groups of the zeolite (see Table 1), (○) CD_mH_{4-m} ($m = 0$–3); (□) SiOHAl; (▷) SiOH. The rate constants k_{SiOHAl} and k_{intra}, which correspond to the solid curves, are given in Table 2.

Table 2
Rate constants of the H/D exchange for methane-d_4 on H-BEA and methane-d_4 and ethane-d_6 on Zn/H-BEA

T/(K)	H-BEA		Zn/H-BEA			
	Methane		Methane		Ethane	
	k_{SiOHAl}[a]	k_{intra}[a]	k_{SiOHAl}[a]	k_{intra}[a]	k_{SiOHAl}[a]	k_{intra}[a]
433			17 ± 1	40 ± 20		
453			55 ± 10	100 ± 60	19 ± 2	60 ± 40
473			140 ± 10	200 ± 100		
488			270 ± 20	350 ± 100	72 ± 8	280 ± 150
508			580 ± 80	650 ± 200	175 ± 25	500 ± 200
528					500 ± 100	850 ± 250
538					800 ± 100	1100 ± 450
548	2.8 ± 0.2	⩾11			900 ± 100	1300 ± 500
553	3.2 ± 0.2	⩾13				
558	4.2 ± 0.3	⩾17				
563	6.3 ± 0.4	⩾25				

[a] $\times 10^6$ (g μmol^{-1} min^{-1}).

due to a transfer of protium from SiOHAl to CD_4 and due to intra-zeolite H/D exchange between SiOHAl and SiOH groups.

Simulation of experimentally obtained kinetic curves for the alkane and both acidic and non-acidic hydroxyl groups (Fig. 5) in accordance to the parallel scheme of the exchange (Table 1) offers the rate constants for both the alkane exchange with Brønsted acid sites and intra-zeolite exchange between SiOH and SiOHAl. The obtained values of k_{intra} are at least 4 times higher than k_{SiOHAl} (Table 2). This is in a good accordance with earlier conclusions that the rate of intra-zeolite exchange is faster than the rate of exchange between zeolite and alkane [17, 49,50]. Since the exchange rate between SiOHAl groups and alkane molecules on zeolite H-BEA is very slow, we were able to estimate only the lower limit for k_{intra}. The Arrhenius plot for k_{SiOHAl} (Fig. 6) gives the activation energy of 138 kJ mol^{-1}, which is in good agreement with values earlier experimentally [17,22,23] and theoretically [17–19,21,24,27,28] obtained for acidic zeolites.

3.5. H/D exchange of methane-d_4 and ethane-d_6 on Zn/H-BEA

^{1}H MAS NMR spectra of methane-d_4 (or ethane-d_6) adsorbed on Zn/H-BEA show similar changes like for methane-d_4

adsorbed on H-BEA. The intensity of the signal from the alkane increases while the intensities of both SiOHAl and SiOH decrease (Fig. 7). A profound difference between the zeolites is that for Zn/H-BEA the exchange is already notable at 430 K. The exchange approaches equilibrium within 20 min at 508 K, whereas for H-BEA this equilibrium would be reached only after 30 days at 508 K.

The kinetics of the H/D exchange was monitored for methane-d_4 and ethane-d_6 in the temperature range of 433–548 K, see Figs. 8 and 9. The obtained values of k_{SiOHAl} and k_{intra} are given in Table 2. For Zn/H-BEA, the rates of the H/D exchange between SiOHAl groups and the alkanes are comparable with rate of intra-zeolite exchange ($k_{\mathrm{SiOHAl}} \sim k_{\mathrm{intra}}$). The rate k_{intra} can be determined with a better accuracy than for zeolite H-BEA. Arrhenius plots of the exchange rate constants versus the reciprocal temperature offer the activation energies for these reactions (Figs. 10 and 11). The activation energies are in the range of 86–88 kJ mol^{-1} for the exchange between

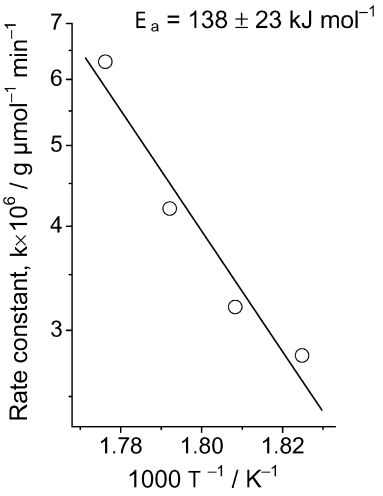

Fig. 6. Arrhenius plot for the reaction of the H/D exchange between methane-d_4 and SiOHAl groups of H-BEA.

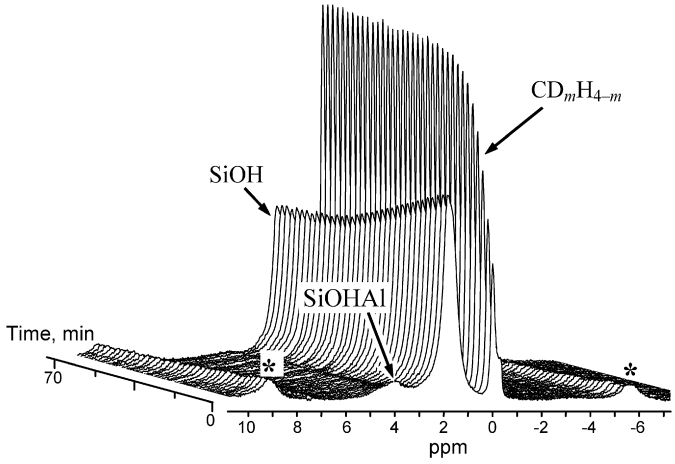

Fig. 7. Stack plot of the ^{1}H MAS NMR spectra at 508 K of methane-d_4 adsorbed on Zn/H-BEA. The time interval between successive spectra recording was 2 min. An increasing signal at 0.0 ppm belongs to methane CD_mH_{4-m} ($m = 0$–3), whereas the decreasing signals at 4.0 and at ca. 5.1 ppm arise from SiOHAl groups. A decreasing signal at 1.7 ppm has mainly a contribution from terminal SiOH. Asterisks (*) belong to the spinning sidebands.

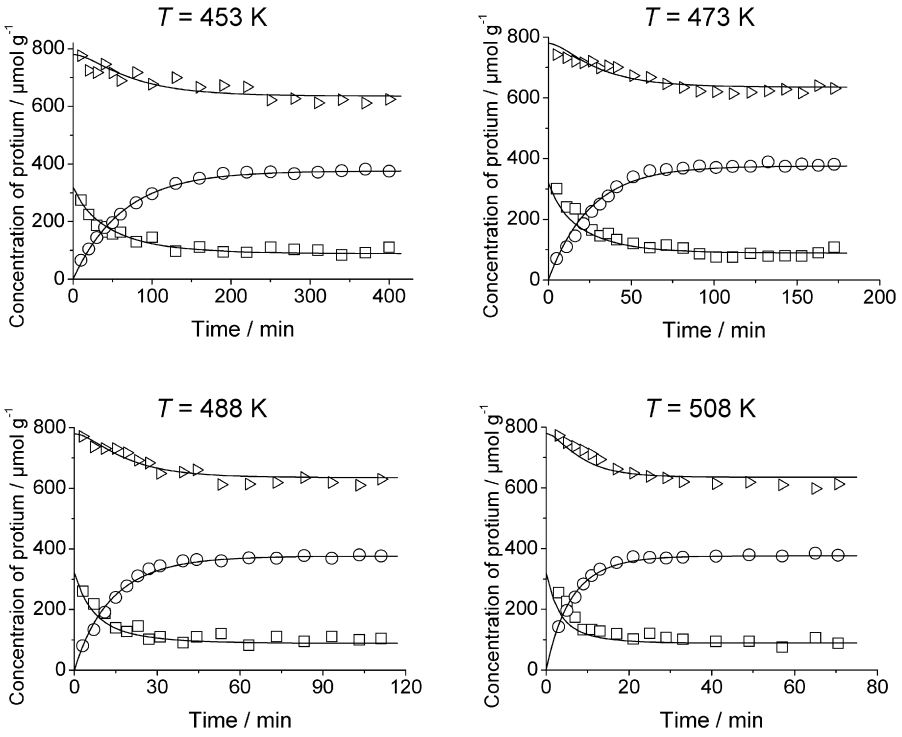

Fig. 8. Experimental and simulated (solid curves) kinetics of the H/D exchange for methane-d_4 on Zn/H-BEA. Simulation was performed in accordance to parallel kinetic scheme of the H/D exchange between SiOHAl and methane and between SiOHAl and SiOH groups of the zeolite (see Table 1), (○) CD_mH_{4-m} ($m = 0$–3); (□) SiOHAl; (▷) SiOH. The rate constants k_{SiOHAl} and k_{intra}, which correspond to the solid curves, are given in Table 2.

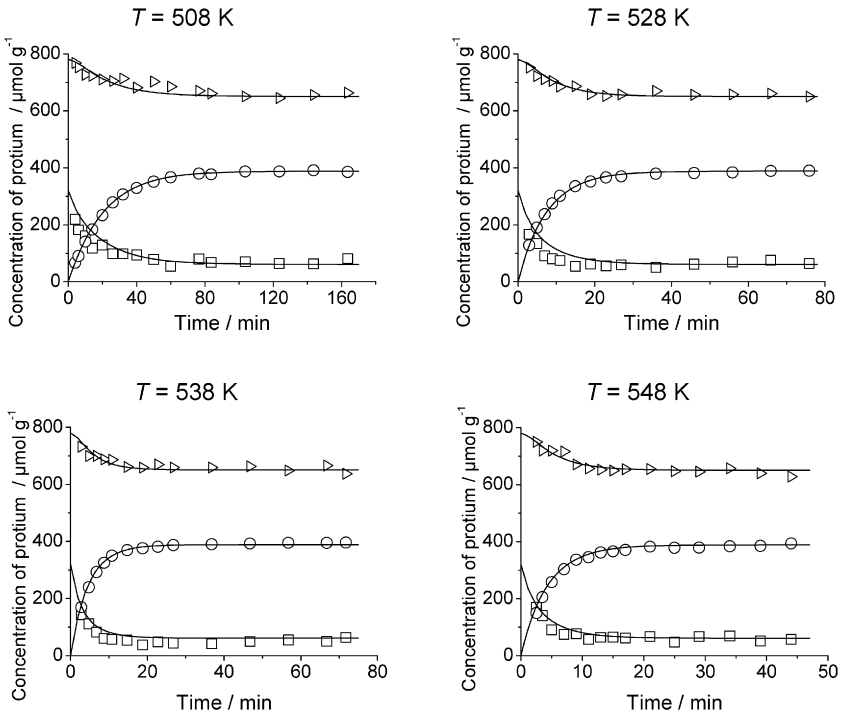

Fig. 9. Experimental and simulated (solid curves) kinetics of the H/D exchange for ethane-d_6 on Zn/H-BEA. Simulation was performed in accordance to parallel kinetic scheme of the H/D exchange between SiOHAl and ethane and between SiOHAl and SiOH groups of the zeolite (see Table 1), (○) $C_2D_nH_{6-n}$ (n = 0–5); (□) SiOHAl; (▷) SiOH. The rate constants k_{SiOHAl} and k_{intra}, which correspond to the solid curves, are given in Table 2.

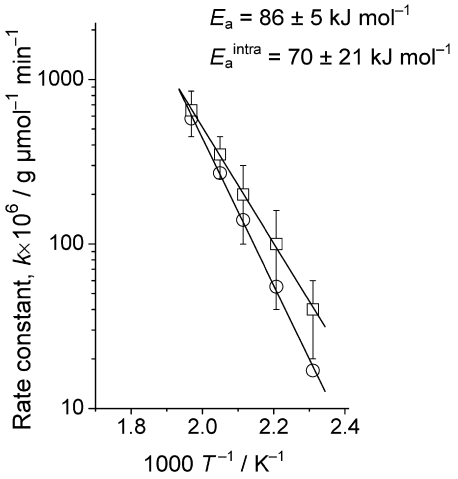

Fig. 10. Arrhenius plots of the H/D exchange for methane-d_4 on Zn/H-BEA, (○) k_{SiOHAl} and (□) k_{intra}. Error bars are shown for k_{intra}.

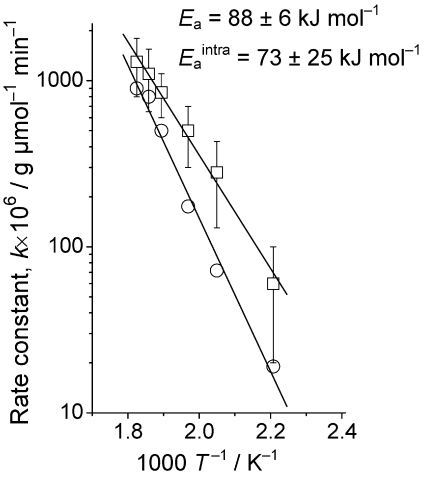

Fig. 11. Arrhenius plots of the H/D exchange for ethane-d_6 on Zn/H-BEA, (○) k_{SiOHAl} and (□) k_{intra}. Error bars are shown for k_{intra}.

the acidic groups of the zeolite and the alkane molecules. They are similar for methane and ethane. The activation energy for intra-zeolite hydrogen exchange is 70 ± 25 kJ mol^{-1}.

4. Discussion

A significant hydrogen exchange between molecules of methane and ethane, as the most inert alkanes, and SiOHAl groups of acidic forms of zeolites can be usually observed within the temperature range of 623–773 K [17,22,23,54]. Terminal SiOH groups are not involved in the exchange [17]. Activation energies are 120–150 kJ mol^{-1} for the exchange of methane and ethane on acidic zeolites [22,23] or silica alumina [54]. The exchange is accepted to occur in a concerted step involving a penta-coordinated carbon atom [17–19,21,24,27,28,55].

For the H/D exchange of methane on H-BEA, we find activation energy of 138 kJ mol^{-1} and a reaction onset above 548 K. It is in good agreement to early studies of the methane exchange on acidic zeolites [22,23]. This allows us to conclude that the mechanism of the exchange involves penta-coordinated carbon atom in a transition state [17–19,21–25,27,28,55].

For Zn/H-BEA, the kinetic parameters of H/D exchange change dramatically. The rate constants k_{SiOHAl} are at least

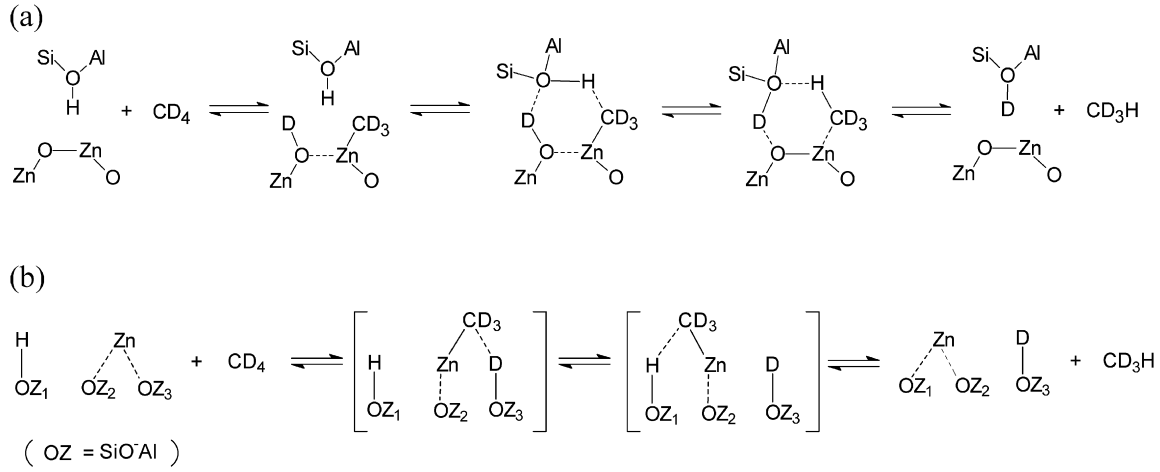

Scheme 1. Possible mechanisms of the H/D hydrogen exchange for methane-d_4 on Zn/H-BEA with involvement of Zn-alkyl species: (a) intermediate Zn-alkyl is formed on ZnO clusters; (b) intermediate Zn-alkyl is formed on Zn^{2+} cations. A similar mechanism can be realized for the exchange with ethane-d_6.

two orders of magnitude higher. The activation energy of 86–88 kJ mol^{-1} is rather low. The exchange proceeds with a notable rate at temperatures at least 100 K lower compared to that on H-BEA. The lower apparent activation energy for the exchange on Zn/H-BEA and the low temperature range of this reaction imply *a promoting effect of Zn* on the reaction of the H/D exchange. The mechanism of the exchange seems to be different from that usually accepted for pure acidic zeolites [17–28,55].

It has been recently shown by IR spectroscopy that adsorption of small alkanes like methane and ethane forms Zn-alkyl species on zeolites Zn/H-ZSM-5 [12–14,56]. Theoretical studies have also indicated a possibility of the formation of Zn-alkyl species during the adsorption of methane and ethane on Zn-loaded zeolites [57,58]. Cross polarization (CP) [59] can enhance NMR signals from strongly adsorbed species. By using ^{13}C CP MAS NMR technique, we could confirm that at temperatures above 473 K a small quantity of Zn-methyl or Zn-ethyl species form on Zn/H-BEA from methane [60] or ethane [60,61]. Kazansky et al. [12–14] have shown that Zn-alkyl species may be formed on Zn^{2+} cations. However, Ivanova et al. [15] demonstrated by NMR and IR spectroscopy that Zn-alkyl species might be also formed from propane on ZnO clusters for the zeolite with large content of the loaded zinc (ca. 8 wt%).

We have recently observed a regioselective H/D exchange for propane on Zn/H-MFI [62]. It has been concluded that the regioselectivity can be rationalized either by the protonation/deprotonation steps with the acidic OH groups of the intermediate propene or by involvement of Zn-alkyl species, which are formed on either Zn^{2+} cations or ZnO clusters [62]. For the exchange of methane on Zn-loaded zeolite, only the involvement of Zn-alkyl species can be realized, since the intermediate alkene cannot be formed from methane. So, Zn promotes the exchange by providing the H/D exchange with involvement of the formed Zn-alkyl species. The analysis of the Zn state in our Zn/H-BEA indicates that both possibilities for the formation of Zn-alkyl species, on either Zn^{2+} cations or ZnO clusters, are plausible. Both Zn^{2+} cations and sub-nanometric ZnO clusters are found inside the pores of Zn/H-BEA (see Section 2).

Scheme 1 shows the possible mechanisms of the H/D exchange for methane (or ethane). This scheme is similar to the mechanism for the regioselective exchange of propane on Zn/H-MFI [62]. Scheme 1a offers the mechanism with involvement of Zn-alkyl species, which are formed on ZnO clusters. Dissociative adsorption of the deuterated alkane on zinc oxide sites (small ZnO clusters, located inside zeolite pores) leads to Zn-alkyl species and Zn-OD groups [15]. Protonation of the zinc-alkyl species by the nearest acidic OH group of the zeolite with synchronous reverse transfer of the deuterium from the ZnOD to the zeolite acid site, provides finally a transfer of protium from the SiOHAl group to the alkane molecule.

Alkane molecules adsorbed on Zn^{2+} cations located at neighbor [63] or distantly separated [64] basic oxygens of $SiO^{(-)}Al$ groups in the zeolite framework can also provide a heterolytic dissociative adsorption of the alkane. It offers the formation of zinc-alkyl fragments and the acidic protons of the SiOHAl group. A reversible formation of zinc alkyl and acidic OH groups from the alkane and Zn^{2+} cations and an involvement of the residual SiOHAl groups of the Zn-loaded zeolite can provide a hydrogen exchange between the adsorbed alkane and SiOHAl groups. Scheme 1b shows a possible mechanism of the exchange for methane (it can also be applied to ethane), which involves Zn-methyl fragments formed on Zn^{2+} cations. In this scheme OZ_2 and OZ_3 represent the basic neighbor or distantly separated oxygens of $SiO^{(-)}Al$ groups in the zeolite framework. HOZ_1 is the residual SiOHAl group that remained in the zeolite after Zn-loading. HOZ_1 groups should be in vicinity of Zn^{2+} cations. In this case, the transition state (depicted in Scheme 1b in square brackets) can be formed, and the H/D exchange can occur.

It should be noted that the H/D exchange is faster for the more inert methane than for ethane: k_{SiOHAl} is ca. three times larger for methane, see Table 2. This may be due to the different stabilities of Zn-methyl and Zn-ethyl species. Indeed, according to theoretical studies by Barbosa et al. [57,58] and Yakovlev et

al. [65] Zn-methyl species should be more stable than Zn-ethyl ones.

5. Conclusion

In situ ^{1}H MAS NMR monitoring of the kinetics of the H/D hydrogen exchange between small alkanes, methane and ethane, and acidic form (H-BEA) and Zn-loaded form of zeolite beta (Zn/H-BEA) allowed us to draw the following conclusions.

Kinetic parameters of the exchange between methane and H-BEA are similar to those earlier obtained for this alkane on acid zeolites. The activation energy is 138 kJ mol^{-1} and the reaction occurs slowly at temperatures in the range 548–563 K. Hydrogen exchange between Brønsted acid sites of Zn/H-BEA and small alkanes (methane and ethane) occurs with a notable rate at a temperature 100 K lower compared to that on H-BEA. The rate of exchange is more than two orders of magnitude higher compared to that on H-BEA. The decrease of the temperature of the reaction and the essentially higher rate and lower activation energy (86–88 kJ mol^{-1}) compared to H-BEA are attributed to the promoting effect of zinc in zeolite. The promotion may consist of involvement of Zn-alkyl species in the exchange. They can be formed either on ZnO clusters or Zn^{2+} cations, located on neighbor or remote $SiO^{(-)}Al$ groups.

Acknowledgments

This work was supported by INTAS (Grant no. 03-51-5286), Russian Foundation for Basic Research (Grant no. 07-03-00136) and the Deutsche Forschungsgemeinschaft, Project FR 902/15.

References

[1] Y. Ono, Catal. Rev. Sci. Eng. 34 (1992) 179.
[2] J.A. Biscardi, G.D. Meitzner, E. Iglesia, J. Catal. 179 (1998) 192.
[3] J.A. Biscardi, E. Iglesia, J. Catal. 182 (1999) 117.
[4] A. Hagen, F. Roessner, Catal. Rev. Sci. Eng. 42 (2000) 403.
[5] Y. Ono, H. Nakatani, H. Kitagawa, E. Suzuki, Stud. Surf. Sci. Catal. 44 (1989) 279.
[6] A. Hagen, O.P. Keipert, F. Roessner, Stud. Surf. Sci. Catal. B 101 (1996) 781.
[7] L.B. Pierella, G.A. Eimer, O.A. Anunziata, React. Kinet. Catal. Lett. 63 (1998) 271.
[8] J.A. Biscardi, E. Iglesia, Catal. Today 31 (1996) 207.
[9] J.A. Biscardi, E. Iglesia, J. Phys. Chem. B 102 (1998) 9284.
[10] E. Iglesia, J.E. Baumgartner, G.L. Price, J. Catal. 134 (1992) 549.
[11] E. Iglesia, D.G. Barton, J.A. Biscardi, M.J.L. Gines, S.L. Soled, Catal. Today 38 (1997) 339.
[12] V.B. Kazansky, A.I. Serykh, E.A. Pidko, J. Catal. 225 (2004) 369.
[13] V.B. Kazansky, E.A. Pidko, J. Phys. Chem. B 109 (2005) 2103.
[14] V.B. Kazansky, I.R. Subbotina, N. Rane, R.A. van Santen, E.J.M. Hensen, Phys. Chem. Chem. Phys. 7 (2005) 3088.
[15] Y.G. Kolyagin, V.V. Ordomsky, Y.Z. Khimyak, A.I. Rebrov, F. Fajula, I.I. Ivanova, J. Catal. 238 (2006) 122.
[16] A. Ozaki, Isotopic Studies of Heterogeneous Catalysis, Kodansha, Tokyo, 1977.
[17] G.J. Kramer, R.A. Van Santen, C.A. Emeis, A.K. Nowak, Nature (London) 363 (1993) 529.
[18] S.R. Blaszkowski, A.P.J. Jansen, M.A.C. Nascimento, R.A. van Santen, J. Phys. Chem. 98 (1994) 12938.
[19] G.J. Kramer, R.A. Van Santen, J. Am. Chem. Soc. 117 (1995) 1766.
[20] J.O.M.A. Lins, M.A.C. Nascimento, J. Mol. Struct. 371 (1996) 237.
[21] P.M. Esteves, M.A.C. Nascimento, C.J.A. Mota, J. Phys. Chem. B 103 (1999) 10417.
[22] B. Schoofs, J.A. Martens, J.P.A., R.A. Schoonheydt, J. Catal. 183 (1999) 355.
[23] B. Lee, J.N. Kondo, F. Wakabayashi, K. Domen, Catal. Lett. 59 (1999) 51.
[24] J.M. Vollmer, T.N. Truong, J. Phys. Chem. B 104 (2000) 6308.
[25] W. Hua, A. Goeppert, J. Sommer, J. Catal. 197 (2001) 406.
[26] S.S. Arzumanov, S.I. Reshetnikov, A.G. Stepanov, V.N. Parmon, D. Freude, J. Phys. Chem. B 109 (2005) 19748.
[27] X. Zheng, P. Blowers, J. Mol. Catal. A Chem. 242 (2005) 18.
[28] X. Zheng, P. Blowers, J. Mol. Catal. A Chem. 246 (2006) 1.
[29] W. Schmidt, A. Toktarev, F. Schueth, K.G. Ione, K. Unger, Stud. Surf. Sci. Catal. 135 (2001) 311.
[30] G. Engelhardt, D. Michel, High-Resolution Solid-State NMR of Silicates and Zeolites, Wiley, Chichester, 1987.
[31] J. Chen, Z. Feng, P. Ying, C. Li, J. Phys. Chem. B 108 (2004) 12669.
[32] E.R.H. van Eck, R. Janssen, W.E.J.R. Maas, W.S. Veeman, Chem. Phys. Lett. 174 (1990) 428.
[33] C.P. Grey, A.J. Vega, J. Am. Chem. Soc. 117 (1995) 8232.
[34] D.B. Ferguson, J.F. Haw, Anal. Chem. 67 (1995) 3342.
[35] E.A. Paukshtis, Infrared Spectroscopy in Heterogeneous Acid–Base Catalysis, Nauka, Novosibirsk, 1992 (in Russian).
[36] E. Bourgeat-Lami, P. Massiani, F. Direnzo, P. Espiau, F. Fajula, T.D. Courieres, Appl. Catal. 72 (1991) 139.
[37] A. Zecchina, S. Bordiga, G. Spoto, D. Scarano, G. Petrini, G. Leofanti, M. Padovan, C.O. Arean, J. Chem. Soc. Faraday Trans. 88 (1992) 2959.
[38] C. Jia, P. Massiani, D. Barthomeuf, J. Chem. Soc. Faraday Trans. 89 (1993) 3659.
[39] I. Kiricsi, C. Flego, G. Pazzuconi, W.O. Parker, R. Millini, C. Perego, G. Bellussi, J. Phys. Chem. 98 (1994) 4627.
[40] L.W. Beck, J.F. Haw, J. Phys. Chem. 99 (1995) 1076.
[41] M. Hunger, S. Ernst, S. Steuernagel, J. Weitkamp, Microporous Mater. 6 (1996) 349.
[42] P.J. Kunkeler, B.J. Zuurdeeg, J.C. van der Waal, J.A. van Bokhoven, D.C. Koningsberger, H. van Bekkum, J. Catal. 180 (1998) 234.
[43] C. Paze, S. Bordiga, C. Lamberti, M. Salvalaggio, A. Zecchina, J. Phys. Chem. B 101 (1997) 4740.
[44] F. Deng, Y. Yue, C.H. Ye, J. Phys. Chem. B 102 (1998) 5252.
[45] C. Paze, A. Zecchina, S. Spera, A. Cosma, E. Merlo, G. Spano, G. Girotti, Phys. Chem. Chem. Phys. 1 (1999) 2627.
[46] J. Penzien, A. Abraham, J.A. van Bokhoven, A. Jentys, T.E. Muller, C. Sievers, J.A. Lercher, J. Phys. Chem. B 108 (2004) 4116.
[47] J.B. Higgins, R.B. LaPierre, J.L. Schlenker, A.C. Rohrman, J.D. Wood, G.T. Kerr, W.J. Rohrbaugh, Zeolites 8 (1988) 446.
[48] M.M.J. Treacy, J.M. Newsam, M.W. Deem, Proc. R. Soc. London A 433 (1991) 499.
[49] J. Sauer, C.M. Kölmel, J.-R. Hill, R. Ahlrichs, Chem. Phys. Lett. 164 (1989) 193.
[50] J. Sauer, H. Horn, M. Häser, R. Ahlrichs, Chem. Phys. Chem. 173 (1990) 26.
[51] S.Z. Roginskii, Theoretical Basis of the Isotopic Methods for the Study of Chemical Reactions, USSR Academy of Sciences, Moscow, 1956 (in Russian).
[52] G.F. Froment, K.B. Bishoff, Chemical Reactor Analysis and Design, Willey, New York, 1979.
[53] J. Villadsen, M.L. Michelsen, Solution of Differential Equation Models by Polynomial Approximation, Prentice–Hall, Englewood Cliffs, NJ, 1978.
[54] J.G. Larson, W.K. Hall, J. Phys. Chem. 69 (1965) 3080.
[55] S.R. Blaszkowski, M.A.C. Nascimento, R.A. van Santen, J. Phys. Chem. 100 (1996) 3463.
[56] V.B. Kazansky, V.Y. Borovkov, A.I. Serikh, R.A. van Santen, B.G. Anderson, Catal. Lett. 66 (2000) 39.
[57] L.A.M.M. Barbosa, G.M. Zhidomirov, R.A. van Santen, Phys. Chem. Chem. Phys. 2 (2000) 3909.
[58] L.A.M.M. Barbosa, R.A. van Santen, J. Phys. Chem. B 107 (2003) 14342.
[59] A. Pines, M.G. Gibby, J.S. Waugh, J. Chem. Phys. 56 (1972) 1776.

[60] On Zn/H-BEA, Zn-methyl species exhibits ^{13}C NMR signal at −20 ppm, and Zn-ethyl species shows two signals at ca. −0.4 ppm (CH_2) and 12.1 ppm (CH_3).
[61] A.G. Stepanov, V.N. Parmon, D. Freude, Kinet. Catal. 48 (2007) 521.
[62] A.G. Stepanov, S.S. Arzumanov, V.N. Parmon, Y.G. Kolyagin, I.I. Ivanova, D. Freude, Catal. Lett. 114 (2007) 85.
[63] M.V. Frash, R.A. van Santen, Phys. Chem. Chem. Phys. 2 (2000) 1085.
[64] G.M. Zhidomirov, A.A. Shubin, V.B. Kazansky, R.A. van Santen, Theor. Chem. Acc. 114 (2005) 90.
[65] A.L. Yakovlev, A.A. Shubin, G.M. Zhidomirov, R.A. van Santen, Catal. Lett. 70 (2000) 175.